A Monthly Time Series of the Potentiometric Surface in the Upper Floridan Aquifer, Northern Tampa Bay Area, Florida, Spanning Three Decades: January 1990-September 2024

By Terrie M. Lee and Geoffrey Fouad August 2025

Prepared for Tampa Bay Water



Prepared by Juturna Consulting



A Monthly Time Series of the Potentiometric Surface in the Upper Floridan Aquifer, Northern Tampa Bay Area, Florida, Spanning Three Decades: January 1990-September 2024

By Terrie M. Lee¹ and Geoffrey Fouad²

Suggested citation:

Lee, T. and Fouad, G., 2025, A monthly time series of the potentiometric surface in the Upper Floridan aquifer, Northern Tampa Bay area, Florida, spanning three decades: January 1990-September 2024. Data products and technical report prepared for Tampa Bay Water (Clearwater, FL) by Juturna Consulting (Tampa, FL), 19hh p.

Report and data products available at: www.swfwmd.state.fl.us/resources/data-maps/hydrologic-data

¹ Department of Natural Sciences, Saint Leo University, Saint Leo, FL, terrie.lee@saintleo.edu

² Department of Geography and Environmental Science, Hunter College, New York, NY, geoffrey.fouad@hunter.cuny.edu

Contents

	n	
Objec	tives	2
Data I	Products	2
Physic	cal Setting	
Methods		
Monit	oring-Well Data Collection	
Estima	ating Missing Daily Groundwater Levels (Gap-Filling)	
Geost	atistical Analysis and Kriging	
Cross-	-Validation Analysis	8
Results		
Monit	oring-Well Data	
Estima	ated Daily and Monthly-Average Groundwater Levels	1
Cross-	Validation Error	12
Montl	hly-Average Potentiometric Surfaces	14
Uncer	tainty in the Monthly-Average Potentiometric Surfaces	16
The Fi	nal Spatial Extent of the Mapping Time Series	1
Summary		1
References	cited	18
Figure 1. Figure 2.	Digital elevation model of the study region in the Northern Tampa Bay area showing streams, US Geological Survey stream drainage basin divides, and Tampa Bay Water well-field properties. The white rectangle shows the extent of the potentiometric-surface analysis. The irregular outline shows the cropped extent of the final potentiometric-surface maps. Modified from Lee and Fouad (2014)	e d 3
Figure 3.	Map of the study area showing the location of 195 monitoring wells used for the analysis, including 13 wells where data collection was discontinued since 2016 or 2023. Also shown a subregions around the 11 well fields used to group wells for the gap-fill analysis (green lines), and the extent of the potentiometric-surface map	
Figure 4.	Maps showing the number of daily water-level observations per month at each groundwater monitoring well in the (A) month with the fewest field observations (December 2022) and (B) month with the most field observations (January 2016) between January 2016 and September 2024	
Figure 5.	Graph showing the percentage of daily groundwater observations from 195 wells that were graph graph month between January 1990 and September 2024	
Figure 6.	Histograms showing the frequency distribution of (A) correlation coefficients and (B) standard errors of the linear equation models used to estimate (gap fill) missing daily values in the 195 wells between January 2016 and September 2024	
Figure 7.	Graphs showing monthly-average groundwater levels in three wells in the Northern Tampa Baarea between January 1990 and September 2024. Well locations are shown in figure 3	
Figure 8.	Map showing the mean monthly absolute cross-validation error at 195 wells from January 20 to September 2024. Well locations and ID numbers are mapped in detail in figure 6 of Lee an Fouad (2014)	d

Figure 9.	Maps showing the months with the (A) lowest and (B) highest monthly average potentiometric-surface elevations, and the (C) average potentiometric-surface elevation between January 2016 and September 2024	
Figure 10.	Graph showing the spatially averaged monthly potentiometric-surface elevation for the map area and for the area inside the eight well-field properties, from January 1990 to September 2024	
Figure 11.	Maps showing months with the (A) minimum and (B) maximum kriging error, and the (C) average kriging error between January 2016 and September 2024	
Figure 12.	Graph showing the spatially averaged monthly kriging error for the map area from January 1990 to September 2024	
Associated Data Products		
Supplemental Data 1 — Well characteristics, January 2016-September 2024		
Supplemental Data 2 — Gap-fill equations, January 2016-September 2024		
Supplemental Data 3 – Monthly-average groundwater elevations in wells, January 1990-September 2024		
Supplemental Data 4 — Kriging parameters, January 1990-September 2024		
Raster Files — Monthly-average potentiometric surfaces and standard errors, January 1990-September 2024		
Animation Files — Animation of potentiometric surfaces and associated kriging errors for user preview		
Appendix 1 — Hydrograph comparisons at four wells recording erroneous zero values		

A Monthly Time Series of the Potentiometric Surface in the Upper Floridan Aquifer, Northern Tampa Bay Area, Florida, Spanning Three Decades: January 1990-September 2024

By Terrie M. Lee and Geoffrey Fouad August 2025

Introduction

For more than three decades, groundwater elevations in the Upper Floridan aquifer, a principal aquifer of the United States, have been routinely monitored in the Northern Tampa Bay area of Florida (fig. 1) (Williams and Kuniansky, 2016). Several hundred monitor wells are maintained, and data are collected by three different stakeholders: Tampa Bay Water, a regional water utility, and two governmental agencies: the Southwest Florida Water Management District, a State agency charged with regulating the use of freshwater resources in the area, and the US Geological Survey (USGS), a federal agency that quantifies the Nation's freshwater resources. All three agencies require unbiased and long-term physical evidence to describe hydrologic conditions in the Upper Floridan aguifer (e.g., Geurink and Basso, 2013; Haag and Lee, 2010; Southwest Florida Water Management District, 1999). To provide this evidence, the USGS in cooperation with Southwest Florida Water Management District created a consensus mapping product using data from the three monitoring networks. The result was an unprecedented time series of highly spatially resolved potentiometric-surface maps describing the monthlyaverage groundwater elevations in the Upper Floridan aguifer over a 573-mi² area covering portions of six stream watersheds and the entirety of 11 Tampa Bay Water well fields (Lee and Fouad, 2014).

The initial mapping time series, which quantified potentiometric-surface elevations in the aquifer for the decade 2000 to 2009, was then extended backward and forward in time to describe 26 years, from 1990 to 2015 (Lee and Fouad, 2017). The 26-year long mapping product described regional groundwater conditions for thirteen years before and thirteen years after large, legally mandated reductions in groundwater pumping were implemented at the 11 well fields (Interlocal Agreement 1998, p. 75). The extended time series was additionally used to evaluate changes in the hydrologic condition of thousands of regional wetlands (Hogg et al., 2020; Lee and Fouad, 2018).

In Florida's permeable karst terrain, spatially distributed potentiometric-surface elevation is a versatile line of physical evidence that can be employed to describe and quantify the groundwater condition in overlying wetlands, lakes, and streams (e.g., Lee et al., 2010; Lee and Fouad, 2014; Lee and Fouad, 2018). For example, the 26-year mapping product was used to calculate a wetland groundwater condition metric that allowed the monthly groundwater condition in thousands of palustrine wetlands in the Northern Tampa Bay area to be compared before and after pumping was reduced in well fields (Lee and Fouad, 2018). The new metric was a corroborating line of evidence to use with observations made in hundreds of wetlands monitored by Tampa Bay Water during that time, and an independent line of evidence to argue the hydrologic recovery in thousands of unmonitored wetlands (Lee and Fouad, 2018; Hogg et al., 2020). The broader applicability of the metric for wetlands in other regions of the US was described by Fouad and Lee (2021).

Seasonal patterns of rainfall are shifting in Florida due to climate change and monthly data on the Upper Floridan aguifer can be used for managing regional groundwater resources. Aggregate groundwater pumping from the 11 Tampa Bay Water well fields in the area has been maintained at around 90 million gallons per day on average since 2008 and will continue at that rate until 2032 (Southwest Florida Water Management District Water Use Permit 11771.002). Within that timeframe, droughts and extreme rainfall events are expected to increase in frequency in the 2010 and 2020 decades compared with the 2000 decade due to climate change (Carter et al., 2018). The 90 million gallon per day annual average rate, shown on figure 2, is computed as a 12-month running average. For this reason, higher monthly pumping rates to meet the water demands of seasonal droughts could predetermine the remainder of the year's pumping regime and increase seasonal drawdown effects at well field properties. At the same time, other, non-Tampa Bay Water groundwater pumping in the Northern Tampa Bay area, mostly for irrigation water demands, may superimpose an added drought effect on regional potentiometricsurface elevations. (Southwest Florida Water Management District, 2025a). Within a given year, increased seasonal drought effects may occur along with greater seasonal wet-season rainfall from tropical storms. Extending the mapping time series beyond December 2015 creates spatially distributed metrics to quantify recent conditions in the Upper Floridan aquifer and to track the hydrologic conditions in overlying surface-water features.

In addition to visualizing monthly climate and pumping effects on groundwater levels, updating the mapping time series reviews the current network of monitoring wells maintained by the three agencies. The analysis catalogs changes in the monitoring network, including the loss or gain of monitoring wells and their sampling frequency; changes that can improve or degrade the accuracy of estimating potentiometric-surface elevations over the map area (Fisher, 2013).

Objectives

This study has two key goals. The first is to analyze groundwater monitoring data collected on the Upper Floridan aquifer in the Northern Tampa Bay area from January 2016 to September 2024 and create a compatible extension to the existing potentiometric-surface mapping time series. Specific objectives of this goal include: (1) describing and characterizing all groundwater monitoring data used for the current analysis; (2) documenting the approach; and (3) summarizing the extreme elevations in the potentiometric surface for this period. The second study goal is to unite the eight year and nine-month-long extension with the previous 26-year long mapping product to create one continuous mapping time series spanning three decades. The resulting downloadable data layers define spatial patterns in the potentiometric surface of the Upper Floridan aquifer in the Northern Tampa Bay area from January 1990 to September 2024, and reveal monthly, seasonal, and annual trends in its elevation for 34 years and nine months.

Data Products

Raster Files – The nearly 35-year mapping time series is packaged in 417 gridded (raster) data layers. Each layer describes one monthly-average potentiometric surface between January 1990 and September 2024 in feet above or below the National Geodetic Vertical Datum of 1929 (NGVD29). The 417 layers reflect 34 years at 12 months per year, and nine months in 2024. The surface elevations are provided as raster grids with x and y cell dimensions of 100 meters and saved as GeoTIFF files for use in a variety of geographic information systems. Another 417 gridded data layers display the estimated standard error in the monthly-average potentiometric-surface elevations in feet. The kriging approach used in this and previous studies by Lee and Fouad (2014; 2017) generates a rectangular

interpolated surface the extent of which is defined by the location of the most northern, southern, eastern, and western monitoring wells in the network (fig. 1). The final maps are clipped smaller than this larger rectangular area to minimize uncertainty in the potentiometric-surface elevations. The final map extent encompasses the greatest concentration of monitoring wells and results in lobed areas around well fields because wells are clustered around the 11 well fields. Kriging error surfaces are in the same gridded format as the potentiometric surfaces. Metadata describing the gridded data products are provided in XML text files accompanying each grid following the Federal Geographic Data Committee Geospatial Metadata Standards. The XML file includes a description of each file and data associated with the file.

Animation Files – One animation file in mp4 format displays the entire potentiometric-surface mapping time series in one-second monthly intervals. The seven-minute-long animation, time adjustable by the user, displays monthly-average potentiometric surfaces between January 1990 and September 2024. Pixels are color-categorized by their elevation values, and elevation contours with a five-foot interval are shown. Well-field property outlines are provided for spatial reference. A second animation displays the spatial distribution of kriging standard error, in feet, of the surface elevations. Previewing both files allows the user to determine the accuracy/uncertainty in the potentiometric-surface elevations in the region where they have a specific interest.

Supplemental data products, described below, are also available for download from the Southwest Florida Water Management District website at https://www.swfwmd.state.fl.us/resources/data-maps/hydrologic-data (see "Other Hydrologic Data Sources"). Besides the supplemental data products provided, two more data tables used for the analysis were provided internally to Tampa Bay Water and can be obtained by request. The first of these is an observed (raw) water-level database containing all available daily observations at the 195 monitor wells from January 1990 to October 2024 (the last month is incomplete). The second is a continuous daily water-level database containing observed and estimated (gap-filled) groundwater elevations in NGVD29 at 195 monitoring wells over the same time period as the raw data.

Supplemental Data 1 – Table 1 identifies and gives physical characteristics of the 195 monitoring wells used in these analyses and the frequency of daily observations at each well between January 2016 and September 2024. Also listed are statistics describing the strength of regression models used to estimate (gap-fill) missing daily water levels and how often a model was used to gap-fill a missing value. The last two columns in Table 1 summarize the mean monthly cross-validation error at each monitor well for the period January 2016 to September 2024.

Supplemental Data 2 – Table 2 is a full account of regression models used to gap-fill missing daily groundwater elevations at the 195 monitor wells. The table

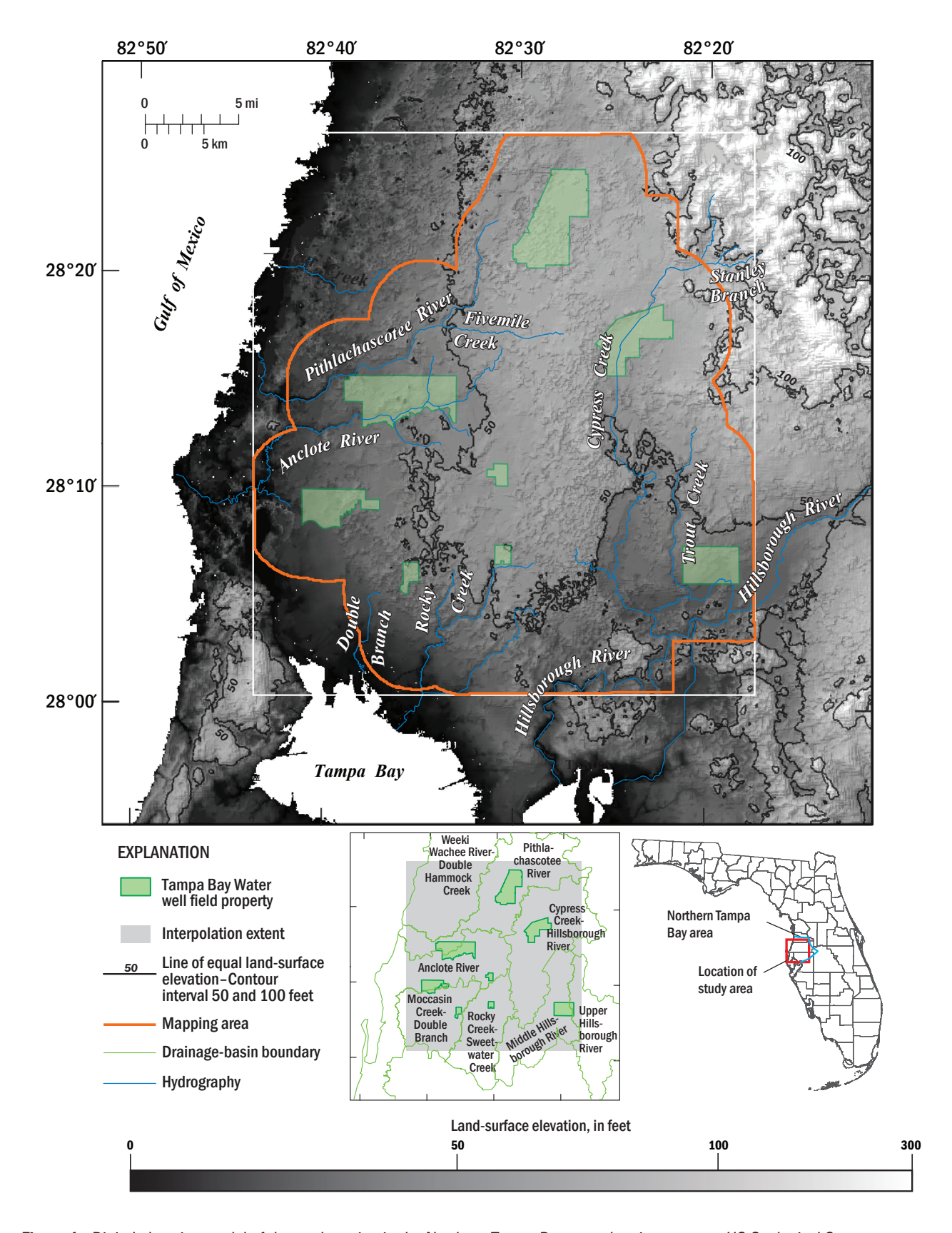


Figure 1. Digital elevation model of the study region in the Northern Tampa Bay area showing streams, US Geological Survey stream drainage basin divides, and Tampa Bay Water well-field properties. The white rectangle shows the extent of the potentiometric-surface analysis. The irregular outline shows the cropped extent of the final potentiometric-surface maps. Modified from Lee and Fouad (2014).

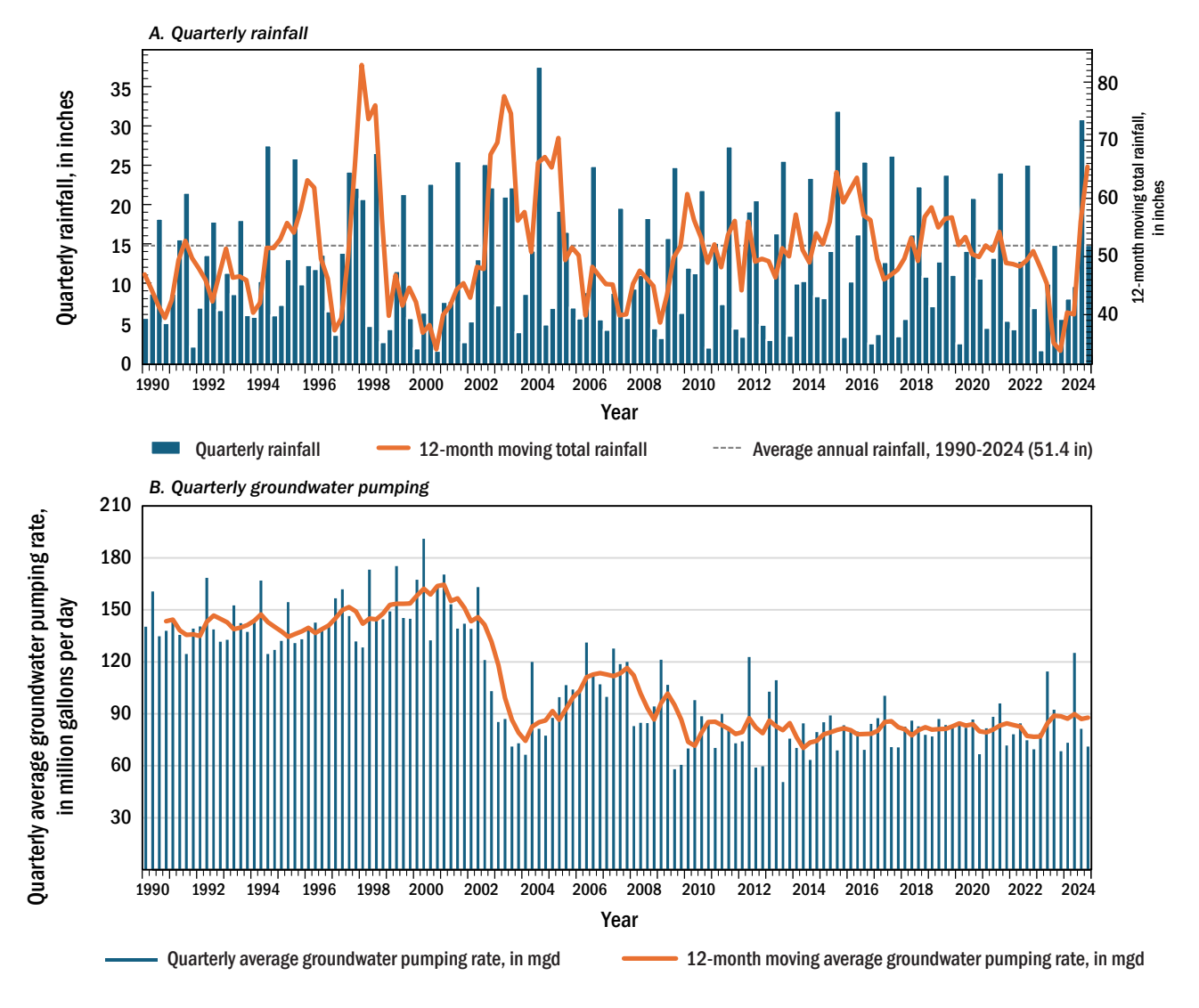


Figure 2. Quarterly (A) total rainfall and (B) average groundwater pumping from the 11 well fields operated by Tampa Bay Water, in the Northern Tampa Bay area from 1990 to 2024.

identifies the cross-correlated predictor well, the size of the sample used in the regression model, the model parameters (i.e., y-intercept and slope), the correlation and R-squared of the model, its standard error in feet, and the frequency of its use both in days used and percentage of days used in the study time period from January 2016 to September 2024.

Supplemental Data 3 – Table 3 summarizes monthly-average groundwater elevations in the 195 wells in NGVD29 feet between January 1990 and September 2024. Monthly-average values are calculated using the gap-filled daily values.

Supplemental Data 4 – Table 4 lists parameters used to curve-fit the monthly hole-effect kriging model semivariograms from January 1990 to September 2024 and cross-validation and standard error statistics expressing the uncertainty of the kriging on a month-by-month basis.

Physical Setting

The Northern Tampa Bay area extends about 30 miles north of metropolitan Tampa, Florida and about 20 miles onshore of the Gulf of Mexico (fig. 1). In this low-lying terrain composed mostly of the Western Valley and Gulf Coastal Lowlands physiographic regions (White, 1970), freshwater wetlands make up over 25 percent of the land area (Haag and Lee, 2010). In the mantled karst geologic setting, the transmissive carbonate formations of the Upper Floridan aguifer are overlain by a thin, semi-confining clay layer and topped by permeable sands and clayey sands (Sinclair et al., 1985). Groundwater from the Upper Floridan aguifer discharges upward along the coastline into springfed rivers that flow into the Gulf of Mexico in Pasco and Hernando Counties. Groundwater recharge predominates farther inland, but inland springs such as Crystal Springs and Sulphur Springs discharge groundwater from the Upper

Floridan aquifer into rivers such as the Hillsborough River which flows into Tampa Bay.

The 12-month moving total rainfall declined overall during the 8-year and 9-month study period from January 2016 to September 2024, (fig. 2a), but increased in the final two quarters of 2024 in response to extreme rainfall from Hurricane Helene on September 26, 2024, and Hurricane Milton on October 9, 2024 (Florida Climate Center, 2024; Southwest Florida Water Management District, 2025b). Annual rainfall for the Tampa Bay coastal area averaged 51.4 inches per year between 1990 and 2024 (Southwest Florida Water Management District, 2025b).

Seasonally, rainfall in the 1st quarter (January to March) of 2023, typically one of the driest quarters of the year, was lower than any quarter in the entire period (fig. 2a). Rainfall in the 2nd quarter of the year (April to June) is typically greater than in the 1st quarter due to the onset of summer rain in June. Yet quarterly pumping rates typically peak in the 2nd quarter of the year because of the large demand for irrigation water in April and May (fig. 2b). This effect is particularly noticeable in the last two years of the extended mapping period, 2023 and 2024. In these years 2nd quarter pumping reached its highest levels in 12 years, since 2012, and the 12-month running total pumping in the well fields was closer to the 90 million gallon per day regulatory maximum than any time since early 2009 (fig. 2b). Precipitation for May 2024 was "drier than normal" in the counties of this study and, according to statistics compiled by the National Oceanic and Atmospheric Administration Climate Prediction Center, May 2024 had the warmest monthly-average air temperature for that month in Tampa since records began in 1890 (3.5°F above normal) (Southwest Florida Water Management District, 2024). Temperatures for May 2025 and April 2025 were their second warmest on record (Southwest Florida Water Management District, 2025c).

Methods

Methods used for the analysis are described briefly in this section, with the emphasis placed on describing minor modifications made to the kriging interpolation approach. The approach applied for this study has been described previously by Lee and Fouad (2017) and the reader is referred there for an expanded description.

Monitoring-Well Data Collection

Monitoring-well data including daily groundwater elevations in the Upper Floridan aquifer in NGVD29 feet were acquired from three data sources: (1) Tampa Bay Water, (2) the Southwest Florida Water Management District, and (3) the US Geological Survey. Tampa Bay Water data were acquired by request on November 6, 2024 (E. Hayes, Tampa Bay Water, written commun., November 2024). Southwest Florida Water Management District and US Geological Survey data were retrieved from the Environmental Data Portal (https://www.

swfwmd.state.fl.us/resources/data-maps/environmentaldata-portal) and the National Water Information System (https://waterdata.usgs.gov/nwis), respectively. Data from the month of October 2024 were incomplete, making the period of the present study January 2016 to September 2024. January 2016 was the first month since the prior potentiometric-surface mapping project (Lee and Fouad, 2017) and September 2024 was the last complete month of available data. Data from the three sources were combined using the maximum value on days when data overlap, following the original format of the data (i.e., daily maximum record). For days before 2016, daily record from the previous project (Lee and Fouad, 2017) were used to preserve backward compatibility with the prior mapping product. All well characteristics are summarized in Supplemental Data 1.

Between January 2016 and September 2024, seven wells were completely without data and six had no data since the start of 2023. Despite their lack of recent data, all 13 well sites were kept in the analysis to preserve compatibility with the previous mapping product and to maintain the original spatial coverage of the network. Synthetic record of groundwater elevations were generated at each well by relying entirely on gapfilling tools. The gap-filled record uses linear regression equations in which the standard error expresses the uncertainty of the gap-filling. To assess the validity of using synthetic record in the current study time period, standard error of the synthetic record at the 13 inactive wells was compared to that of active monitoring wells. The median standard error of active wells was 0.60 feet compared to 0.64 feet for the inactive wells. On taking a random sample of 13 active wells and repeating this process 10,000 times, the median standard error ranged from 0.58 feet to 0.67 feet, meaning the standard errors of active versus inactive wells were comparable. For this reason, synthetic record was used at no-longer active monitoring wells to preserve backward compatibility with the previous mapping product.

Groundwater level observations were collected at differing frequencies in each well. Frequencies ranged from a single monthly field observation to continuous hourly measurements by data loggers from which a daily maximum value was derived. Observations describe potentiometric-surface elevations in the Upper Floridan aquifer at the well location. The frequency of observations is described in Supplemental Data 1 as the percentage of all days with observations during the extended study period, and the average number of daily observations per month during that period. "Well name" in this table is the common identifier used in all the project's supplemental data tables (i.e., for the purpose of joining datasets).

Estimating Missing Daily Groundwater Levels (Gap-Filling)

Gap-filling is the process of estimating missing daily groundwater levels for the purpose of calculating monthlyaverage potentiometric-surface elevations at monitoring

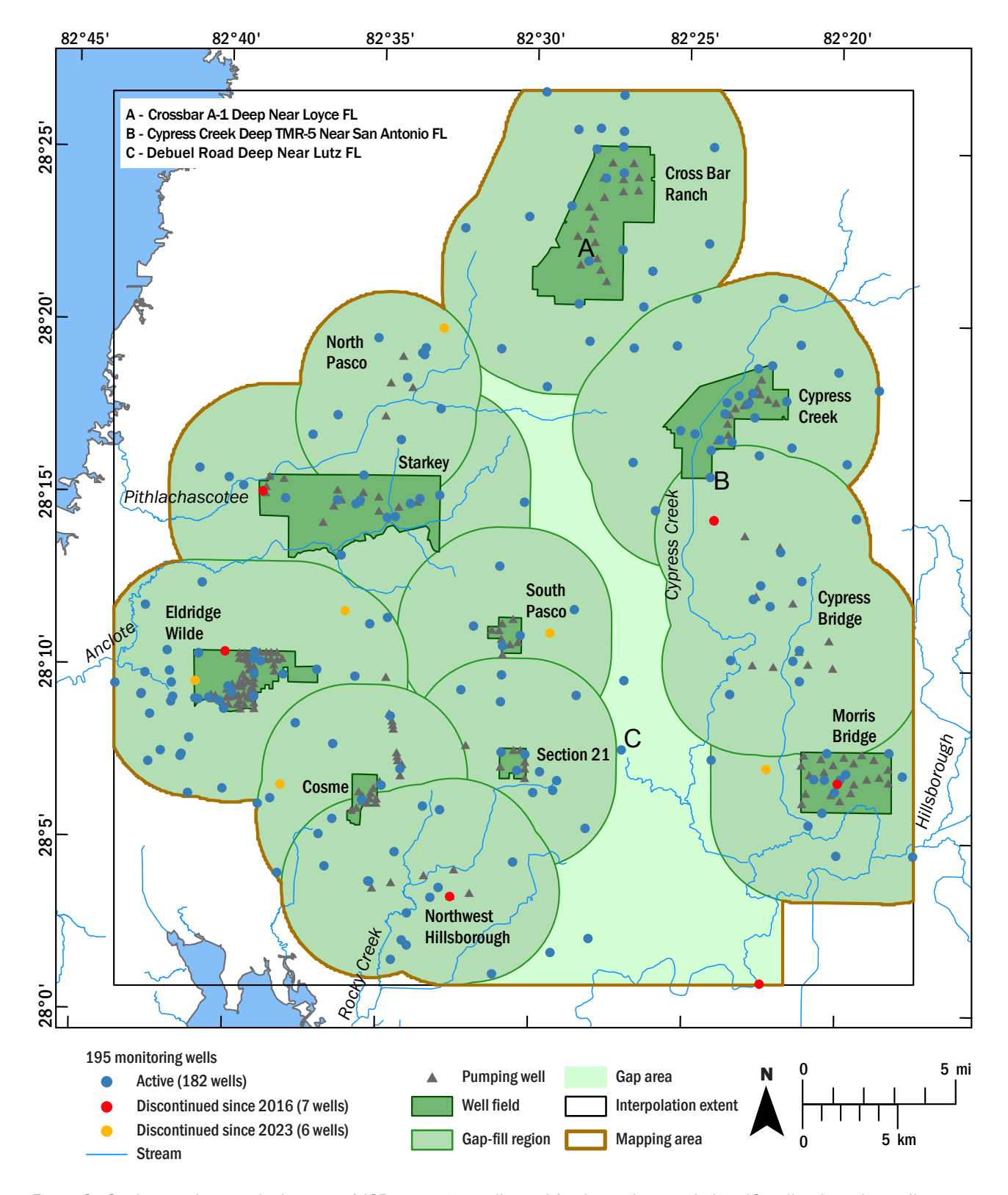


Figure 3. Study area showing the location of 195 monitoring wells used for the analysis, including 13 wells where data collection was discontinued since 2016 or 2023. Also shown are subregions around the 11 well fields used to group wells for the gap-fill analysis (green lines), and the extent of the potentiometric-surface map.

wells. Missing daily observations were estimated (gapfilled) by correlating observed groundwater levels in a subject well to the levels observed in nearby wells and using the best-fit linear equations describing those correlations to predict the missing levels (Conrads et al., 2014).

The daily record was regressed against that of monitoring wells belonging to the same sub-region (fig. 3) to formulate a linear regression model of the form:

$$M_{td} = (\beta_0 + \beta_1 O_{pd})_{md}$$

where M is the missing value of the target well t on day d and the regression model m on day d that has the greatest correlation (Pearson's r) and a standard error of three feet or less is applied including the observation O from the predictor well p on day d multiplied by the regression slope β_1 and adjusted by the y-intercept β_0 . Wells that fall outside of a sub-region are assigned to the nearest one. The purpose of the sub-regions is to group wells subject to similar pumping effects.

For consistency with the results of the earlier 26year time series (Lee and Fouad, 2017), the regression equations based on data from 1990 to 2015 were used for gap filling the missing daily values in this study. Before doing this, however, a comparison was first made between the correlation equations derived using these 26 years of observations and those derived using observations for the entire 34-year and 9-month period. In the process of making this comparison, four wells were discovered to have zeros in the 26-year record where missing values should have been. The source of these zeros was from what are named "permittee supplied" record from the Southwest Florida Water Management District. The zeros in these four wells occurred in data acquired for extending the original potentiometric-surface maps (Lee and Fouad, 2017), not in data for the original study period from 2000 to 2009 (Lee and Fouad, 2014). Zero values in the four wells were found at varying times and in 11 different months (June 2004, August 2004, November 2004, December 2005 to May 2006, and September and October 2015) (see Appendix 1). Most occurred in two co-located Cypress Bridge (CYB) wells. Zero values were replaced with missing values, and the gap-fill regression models for the 26-year period were re-calculated for the four wells below:

ROMP CB-2N Masaryktown Canal FLDN Well, CYB-CYX-1-AP, CYB-CYX-1-SUW Well Near Land O' Lakes FL, and Morris Bridge Deep 13 Near Branchton FL.

Regression equations for the four updated wells, and the remaining wells in the 26-year period, were then compared to the equations formed using corrected observations for the entire 34-year and 9-month period.

The new versus pre-existing gap-fill equations

from Lee and Fouad (2017) are compared in a similar fashion as inactive and active monitoring wells using the regression standard errors and 10,000 random samples. In this case, sampling occurs in the new equations following the two-thirds rule (Efron and Tibshirani, 1997) in which 119 of 178 gap-filled wells are randomly drawn. Median standard errors of the samples range from 0.60 to 0.64 feet. The same statistic of the pre-existing equations falls within that range at 0.63 feet, signifying the pre-existing equations are similar to those of the longer time period and acceptable for use in the present study. The preexisting equations are therefore used in the gap-filling of this study and the subsequent mapping time series spanning the three decades. For an account of the preexisting gap-fill equations applied in this study, the reader is directed to Supplemental Data 2 in which equation parameters are listed and can be re-applied for personal use.

Geostatistical Analysis and Kriging

As in previous studies, a geostatistical analysis approach was used to interpolate the potentiometric surface elevations between the point-values of monthlyaverage elevations at wells. Gap-filled daily values were converted to monthly-average values at each monitoring well (see Supplemental Data 3) and then analyzed in the Geostatistical Analyst extension of ArcGIS Pro 3.1. Ordinary kriging was chosen as the geostatistical method because it models the spatial autocorrelation (i.e., stronger relation between closer points) that commonly occurs in groundwater levels. The spatial autocorrelation of monthly-average groundwater levels was examined after removing the effect of a regional trend in the potentiometric surface. The Upper Floridan aquifer drains from the Brooksville Ridge in the northeastern part of the study area towards the west coast. A second-order polynomial in all directions (i.e., isotropic) fit the regional trend in a previous study of the same area (Lee and Fouad, 2014) and is re-applied here to detrend the data for subsequent modeling of the spatial autocorrelation. Detrending leaves a more normal distribution of groundwater levels required to later map the kriging standard error (or variability in the potentiometric surface).

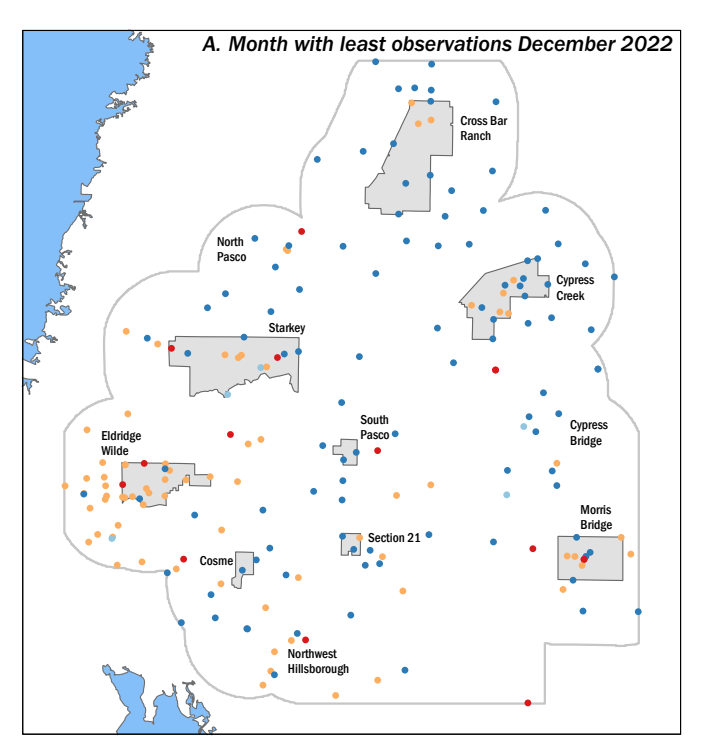
The spatial autocorrelation within each set of monthly-average groundwater levels was modeled using a semivariogram. A semivariogram plots the difference in groundwater levels between every pair of wells on the y axis as semivariance and the distance between every pair of wells on the x axis. The semivariogram modeling of the present project follows the same routine as Lee and Fouad (2017) and the reader is directed there for a fuller account of the method. Briefly, the empirical semivariogram is modeled using a curve called the "hole effect" functional form in ArcGIS. This functional form was previously chosen because it models the periodicity of observed semivariance wherein groundwater levels are more similar around the margins

of physical features such as topographic high points and around the "cones of depression" known to occur in the potentiometric surface around pumping wells (Tampa Bay Water, 2013). The parameters defining the best-fit hole effect curve are calculated each month using a cross-validation process in which each well is omitted from the analysis sequentially. The monthly curve-fit parameters of the hole effect model minimize the error of the cross-validation process and are provided for reproducibility in Supplemental Data 4.

The resulting semivariogram models are the basis of potentiometric-surface interpolations and the standard deviation of observed semivariance around the fitted curve is used to map the kriging standard error, an important metric in expressing the uncertainty of the potentiometric surface elevations. Potentiometric and standard error surfaces each use the same grid dimensions as the previous project (Lee and Fouad, 2017) of 100-meter grid cells. The spatial resolution was justified by the density of the monitoring wells and achieves the end goal of relating the potentiometric surface to small surfacewater features like wetlands. Monthly potentiometric surfaces were kriged for the entire 34-year and 9-month period. Minimum and maximum monthly surfaces were chosen based on the smallest and largest spatially averaged elevation for the map area, respectively.

Cross-Validation Analysis

A cross-validation analysis was applied to indicate the potential for the kriging to over-smooth the interpolated potentiometric-surface elevations between the monitoring-well locations. In a crossvalidation analysis, over-smoothing is inferred if, when the known elevations at a given well are removed from the kriging analysis, the modeled value at that location are notably higher or lower. The analysis is done systematically by omitting the known elevation value at a monitor well from the kriging, then interpolating the potentiometricsurface elevation at that location using surrounding wells. The cross-validation error is calculated as the difference between the interpolated and (minus the) known value. A positive difference is an overestimate, a negative difference is an underestimate, and the greater the magnitude of the absolute difference, the greater potential for over-smoothing. This process was repeated for each monitoring well for each of the monthly surfaces. The period-of-record mean cross-validation error for each well is summarized in the last two columns of Supplemental Data 1. Monthly mean cross-validation errors for each well are shown in Supplemental Data 4. Other statistics like relative error (i.e., crossvalidation error divided by the actual value) and cross-validation standard error (i.e., kriging standard



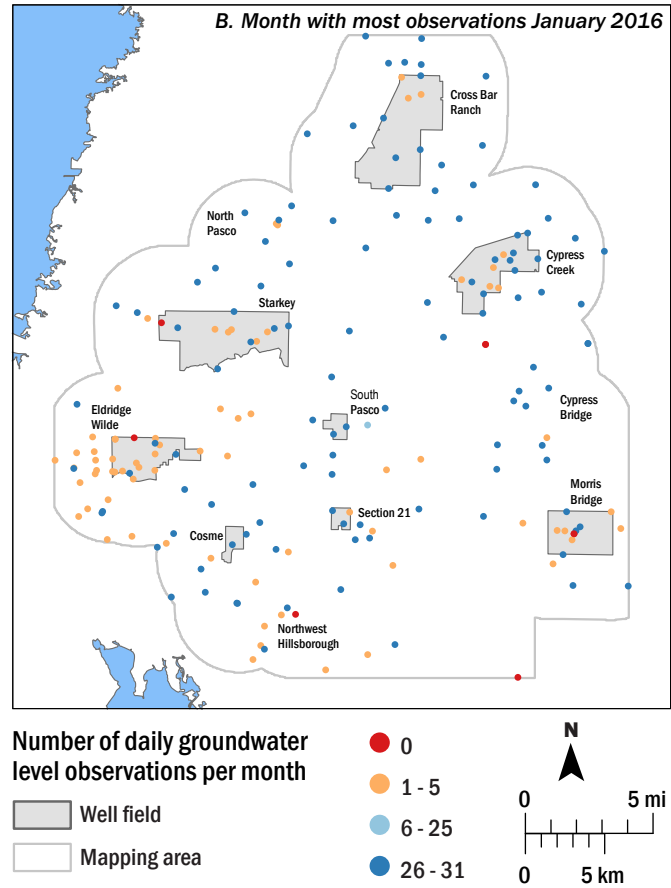


Figure 4. Number of daily water-level observations per month at each groundwater monitoring well in the (A) month with the fewest field observations (December 2022) and (B) month with the most field observations (January 2016) between January 2016 and September 2024.

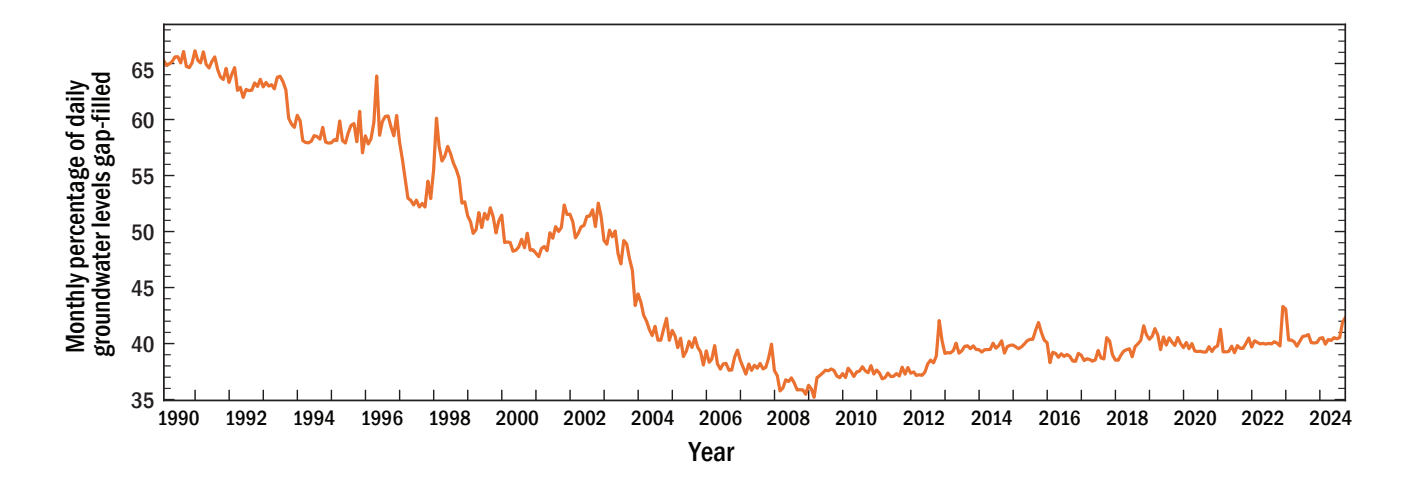


Figure 5. Percentage of daily groundwater observations from 195 wells that were gap filled each month between January 1990 and September 2024.

error on omitting each well) are in Supplemental Data 4 for other assessments of uncertainty.

Results

Monitoring-Well Data

The physical characteristics of the 195 monitoring wells used in this study are summarized in Supplemental Data 1. The table lists the beginning and end dates of the data collected since January 2016 and the percentage of daily data available between January 2016 and September 2024. The well index numbers and names are those used in Lee and Fouad (2014; Appendix 1) and are directly referenceable to all maps and tables provided in the report.

A total of 13 monitoring wells in the network of 195 wells have stopped reporting data in the study time period, leaving 182 wells currently active. Seven network wells do not have data in the study time period (fig. 3), two of which (CYB-CYX-1-AP and CYB-CYX-1-SUW Well Near Land O' Lakes FL) are nearly co-located south of Cypress Creek well field. Another six wells stopped collecting data at various times during the study time period, with record ending as late as 2022 (i.e., wells discontinued since 2023). These 13 inactive wells were part of the earlier mapping products and so were kept in the network of this analysis for consistency. Beyond the dates that these wells have gone inactive, their record was gap-filled using regression equations of comparable standard errors as those used at active wells. The median standard error of equations applied at inactive wells was within the range of median standard errors from 10,000 random samples of active wells. Further, 48 of 182 active wells have gap-filled record exceeding the length of the current study time period (e.g., gap-filled record before well installation in an earlier time period).

The number of daily water-level observations collected per month at individual monitoring wells, also

called the temporal data density, varied widely across the monitoring network between January 2016 and September 2024 (fig. 4). January 2016 had the greatest percentage of daily observations of any month during the mapping period (fig. 4b). In this month, seven wells have zero observations – the seven wells without data for the entire study period. Two of these seven wells are co-located south of Cypress Creek well field, giving the appearance in figure 4b of six wells with zero observations.

December 2022 had the lowest percentage of daily observations. By this month, 13 of the wells in the initial network were not collecting data and had zero observations per month (see red markers, fig. 4a). Groundwater levels had stopped being reported in these 13 wells, either in 2015 or by late 2022 as shown in fig. 3. The absence of daily observations at a well in a month could have also indicated an instrument failure. One to five daily water-level observations per month in a well typically reflected monthly or twice per month measurements collected by hand (fig. 4, orange markers). Monitoring wells with 26 to 31 daily water-level observations per month reflect automated, continuous daily observations (fig. 4, dark blue markers). At relatively fewer sites the number of daily observations was between 6 and 25, a condition that typically reflected continuous daily monitoring at a well that was interrupted by mechanical problems or power interruptions (fig. 4, light blue dots).

During the current mapping period (January 2016 to September 2024), about 58% of all wells in the network (113 of 195 wells) reported daily observations for greater than 90 percent of the possible days. Another 37% of the wells (73 of 195 wells) reported daily observations for 10 percent or less of the possible days (see Supplemental Data 1). This category includes wells with a collection frequency of about 3 or 6 percent, i.e., water levels

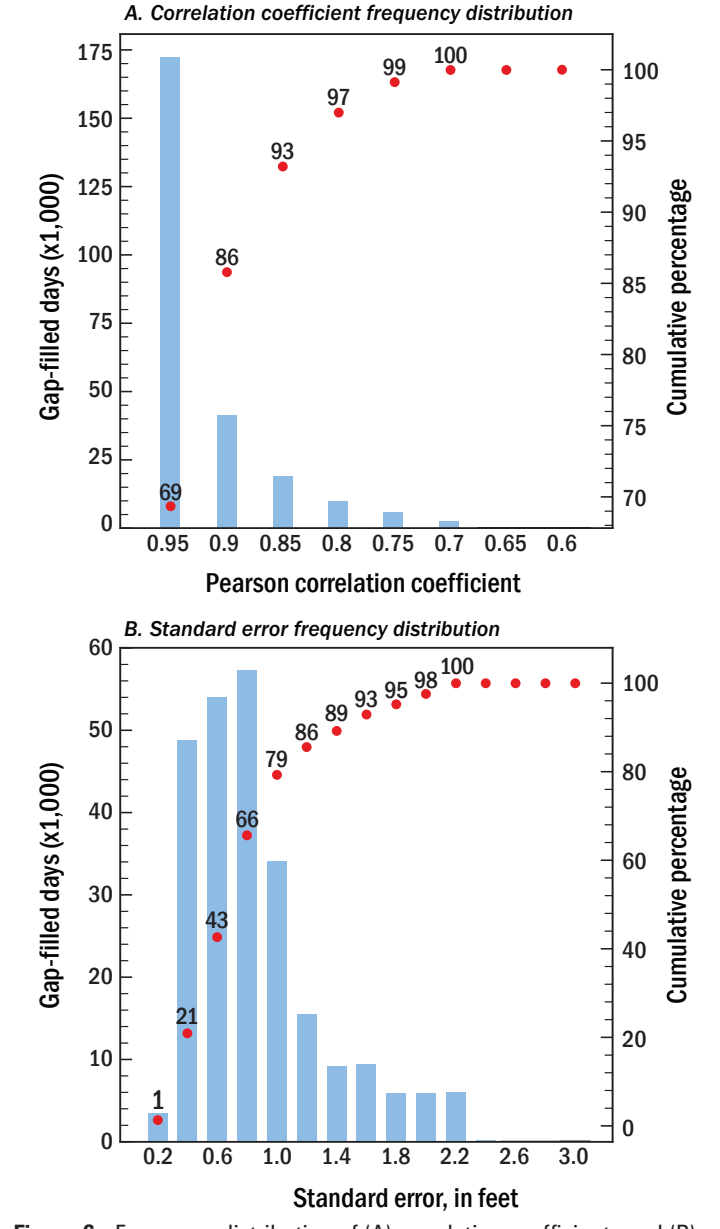


Figure 6. Frequency distribution of (A) correlation coefficients and (B) standard errors of the linear equation models used to estimate (gap fill) missing daily values in the 195 wells between January 2016 and September 2024.

measured once or twice a month, respectively. The remaining 5% of wells (9) had between 10 and 90 percent of daily observations.

The temporal data density across the network was marginally greater than during the preceding five years 2010 to 2015 (Lee and Fouad, 2017; fig. 7). Namely, two more wells made observations at greater than 90% frequency in the current period and five fewer wells collected at a frequency less than 10%. The percentages of daily readings available at each well during the current mapping period are listed in Supplemental Data 1. Five of the 13 wells deactivated during the study period had previously reported near-daily record and would have further increased this margin (Lee and Fouad, 2017).

The temporal data density was greatest in wells around

the Cross Bar Ranch, Cypress Creek, and Cypress Bridge well fields, even when the network reached a minimum number of daily observations per month (compare fig. 4a and b), a finding consistent with earlier studies (Lee and Fouad, 2014 and 2017). By contrast, the temporal data density was lowest in wells around the Eldridge Wilde well field (fig. 4), a condition reported in previous studies (Lee and Fouad, 2017). Spatially, four wells were dropped from the network around Eldridge Wilde well field during the current mapping period, two were on the well field property boundary and two were in the surrounding buffer area (fig. 3).

The percentage of missing daily water-level observations in the well network has continued to increase during the recent study period, after showing a large decline between 1990 and 2008 (fig. 5). During 2008 about 35 percent of daily values in the network were gap-filled, a minimum in the period of record. Nearing the end of 2024 the percentage of all daily observations that were estimated was slightly above 40 percent, with a peak of 46 percent of daily observations gap-filled near the end of 2022.

Supplemental Data 2 provides detailed information on the gap-filling equations. The names of the predictor wells that were highly correlated with each subject well, and used to predict its missing values, are listed along with the equation for each predictor well, its correlation coefficient and standard error of estimate in feet (Supplemental Data 2).

For the period January 2016 to September 2024, about 93% of the estimated daily values used for gap filling were predicted using linear equations with Pearson correlation coefficients of 0.85 or greater and standard error of estimates of 1.6 feet or less (fig. 6). Nearly all (99 percent) of the equations applied have correlation coefficients of 0.75 or greater. The predictive accuracy of equations used for the January 2016 to September 2024 period was comparable to that in earlier studies by Lee and Fouad (2014; 2017).

In the prior project (Lee and Fouad, 2017) two monitoring wells (CYB-CYX-1-AP and CYB-CYX-1-SUW Well Near Land O' Lakes FL) had missing monthly averages because there were no available equations with a standard error of three feet or less to estimate the missing values. However, the large standard errors in correlating these wells to nearby wells were a symptom of these wells having erroneous zeros in their record. With the erroneous zeros omitted in the present work, these two wells now have a complete sequence of monthly averages provided in Supplemental Data 3. These two nearly co-located wells are at a strategically important location between the Cypress Creek stream channel and a production well with no wells nearby (fig. 3),

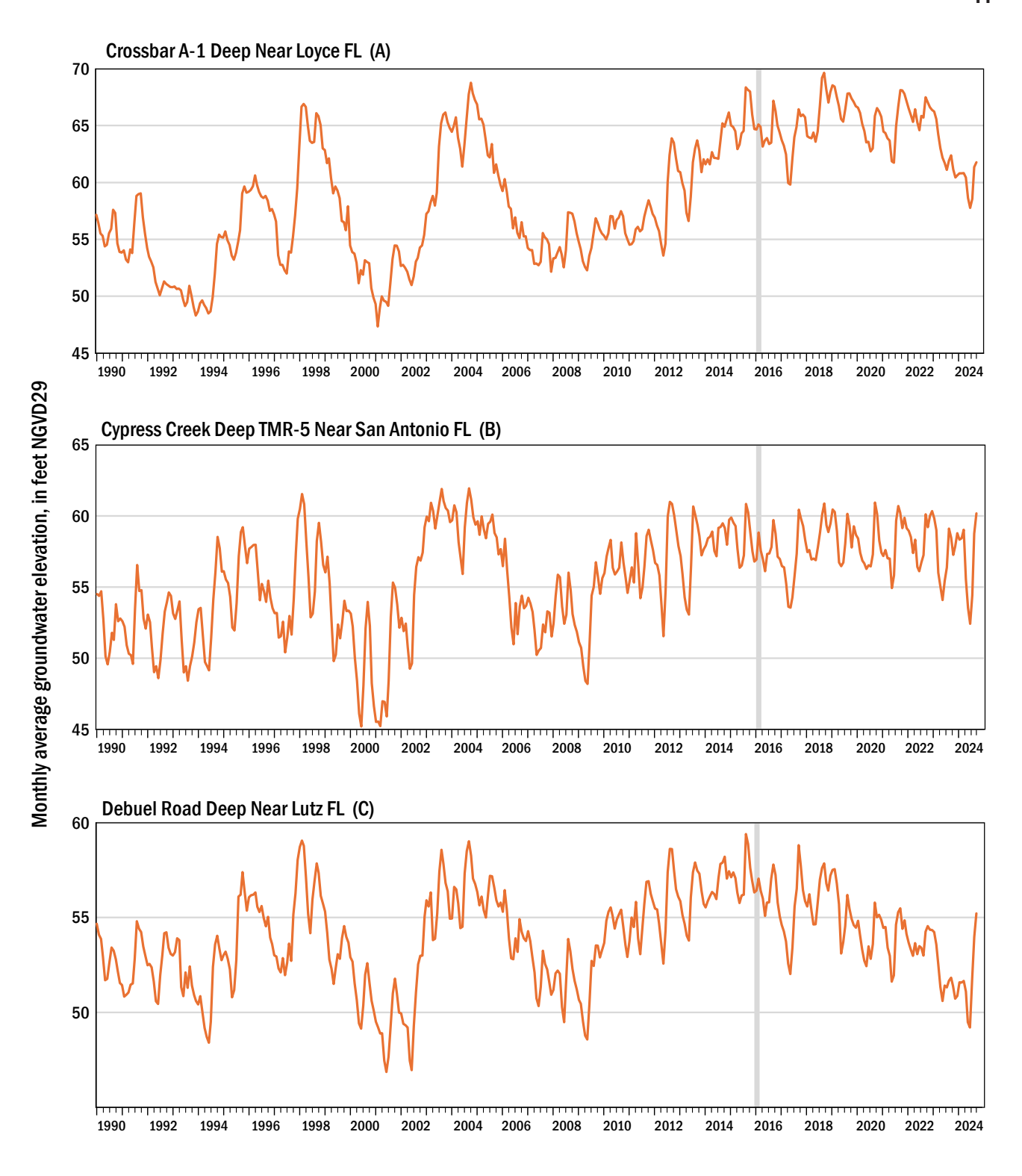


Figure 7. Monthly-average groundwater levels in three wells in the Northern Tampa Bay area between January 1990 and September 2024. Well locations are shown in figure 3.

making this a notable enhancement of the present work. The monthly averages of the two wells are now included in the mapping of the potentiometric surfaces.

Estimated Daily and Monthly-Average Groundwater Levels A continuous daily water-level dataset containing

observed and estimated groundwater elevations in NGVD29 feet was created for 195 monitoring wells for the period January 2016 to September 2024. Daily values then were averaged to generate monthly-average groundwater elevations at each well for the kriging interpolation. Monthly-average elevations were appended

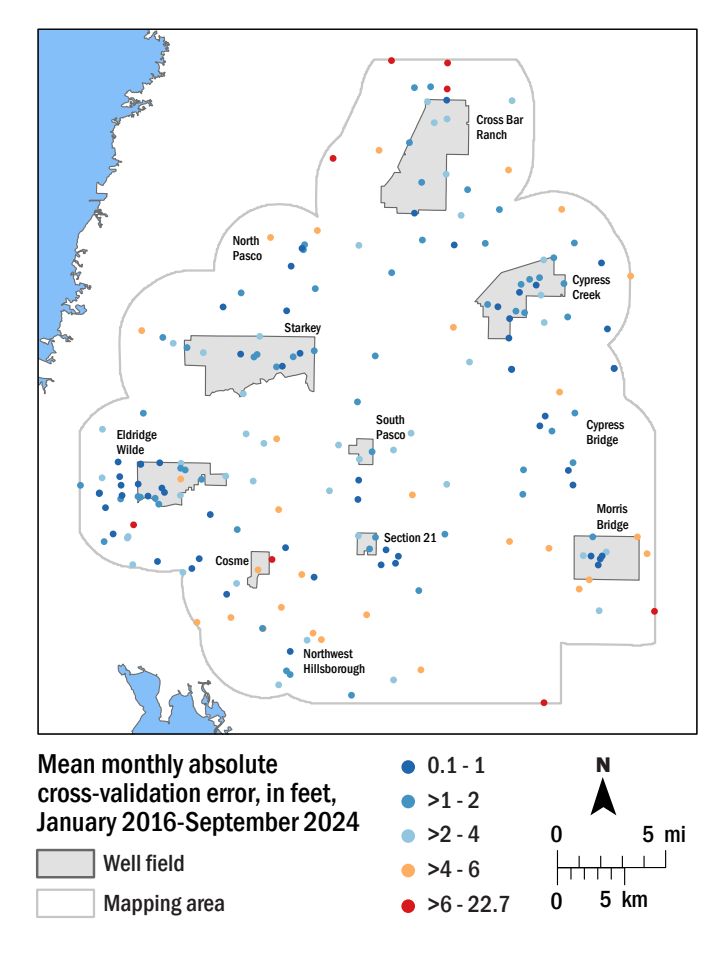


Figure 8. Mean monthly absolute cross-validation error at 195 wells from January 2016 to September 2024. Well locations and ID numbers are mapped in detail in figure 6 of Lee and Fouad (2014).

to record from January 1990 to December 2015 from Lee and Fouad (2017) for all 195 wells. This updated dataset for daily and monthly average values of groundwater elevation spans three decades and corrects the effect of erroneous zero values at four wells: ROMP CB-2N Masaryktown Canal FLDN Well, CYB-CYX-1-AP, CYB-CYX-1-SUW Well Near Land O' Lakes FL, and Morris Bridge Deep 13 Near Branchton FL. At these four wells, missing daily values have been gapfilled using new equations resulting in new monthly average values for the entire period. A dataset of monthly-average groundwater elevations for 195 wells now exists for 34 years and nine months (Supplemental Data 3).

Monthly-average groundwater elevations for three representative wells in the center of the map area showed an overall downward trend between January 2016 and June 2024 after having steadily increased from 2007 to 2015 following well-field pumping cutbacks (fig. 7; well locations shown on fig. 3). The lowest monthly-average elevation of each year trended slightly downward, with the lowest average elevation occurring in June of 2024. Monthly average groundwater levels in all three wells rose steeply upward in September 2024, likely in response to above-average rainfall from Hurricane Helene and reduced pumping (fig. 7 and fig. 2).

Cross-Validation Error

Cross-validation differences or errors were computed for the extended mapping period January 2016 to September 2024 and indicated the relative importance of various monitoring wells for accurately describing the potentiometric surface. The last two columns in Supplemental Data 1 list the mean monthly cross-validation error at each well to reveal under- and overestimates, the absolute cross-validation error at each well gives the magnitude of uncertainty. The identical or nearly identical magnitude of the mean value and mean absolute value for most wells indicates the smoothing bias at a well was consistently either positive or negative for all 105 months.

Of the 195 monitoring wells in the network, the majority (117 wells) had mean monthly absolute crossvalidation errors for the eight-year and nine-month period that were less than 2 feet (fig. 8). Of these, 58 wells had absolute cross-validation errors that were less than 1 foot. At the other extreme, 8 wells had absolute cross-validation errors greater than 6 feet. These larger cross-validation errors can indicate a well with anomalous readings, or more likely, the absence of neighboring wells experiencing the same local phenomenon. The absence of neighboring wells experiencing similar groundwater elevations can reflect insufficient neighboring wells within a large area such as occurs in the southeastern area of the map, or too few wells in a small area where water levels differ greatly on a smaller scale, such as near cones of depression around pumping wells (fig. 8) (Lee et al., 2009).

Five of the eight wells with cross-validation errors greater than 6 feet are located near the edge of the map where pumping stresses are lower, but where wells lack surrounding wells (fig. 8 and wells 3, 5, 7, 160, and 165 in Supplemental Data 1), a pattern previously observed in Lee and Fouad (2014). Four of the wells with cross-validation errors greater than 6 feet are near Cross Bar Ranch well field (1, 3, 5, 7) and speak to the need for additional monitoring wells north and west of Cross Bar Ranch well field (fig. 8). Two of these have the largest cross-validation errors in the well network (well 5 with a mean absolute error of 22.7 feet and well 7 with an error of 11.0 feet).

The southeastern map border has two wells (160 and 165), both shown to have large cross-validation errors and sparce neighbor well coverage in previous studies (Lee and Fouad, 2014 and 2017), and mean absolute cross-validation errors greater than 6 feet in this study (fig. 8). The three stakeholder organizations may consider adding Upper Floridan aquifer monitoring wells to this region of the map, such as locations around the city of Temple Terrace well field where some 14 Upper Floridan aquifer monitoring wells were drilled by the US Geological Survey for a study in the early 2000s (Katz et al., 2007; Table 1). Adding elevation data for these wells and reactivating

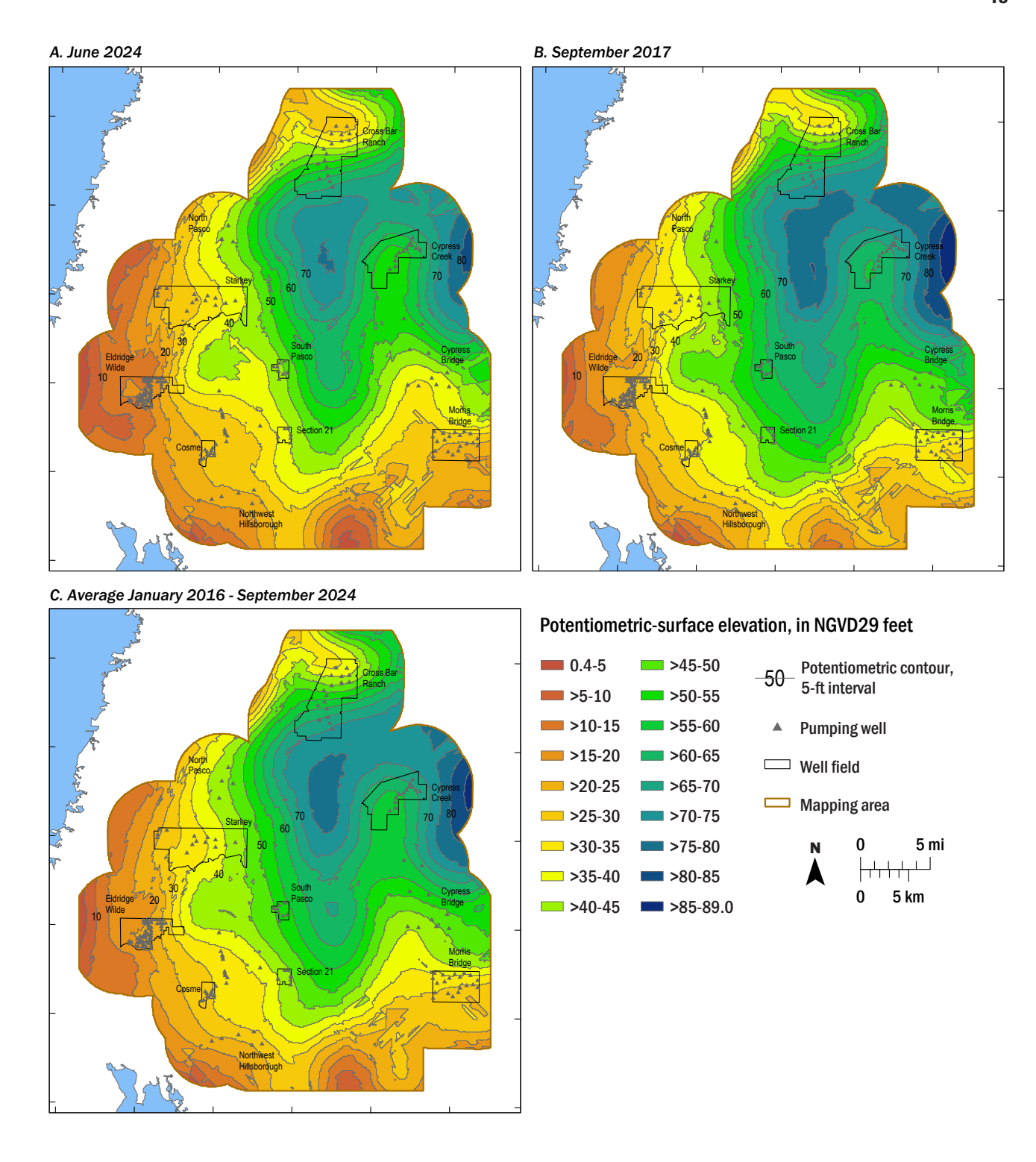


Figure 9. Months with the (A) lowest and (B) highest monthly average potentiometric-surface elevations, and the (C) average potentiometric-surface elevation between January 2016 and September 2024.

monitoring well 174 or 175 from Lee and Fouad (2014), south of Morris Bridge well field, would probably reduce the cross-validation errors in wells 160 and 165, as well as the kriging error of estimating potentiometric surface elevations in the southeastern region of the map.

Finally, two wells (73 and 121) with large cross-validation errors are in the interior of the map by Cosme

and Eldridge Wilde well field properties, respectively (fig. 8 and fig. 6 in Lee and Fouad, 2014). Here large cross-validation errors suggest each well was documenting pumping effects their neighboring wells did not, suggesting additional neighbor wells may be needed to better describe the surface in this area of the map, as discussed in Lee and Fouad (2014).

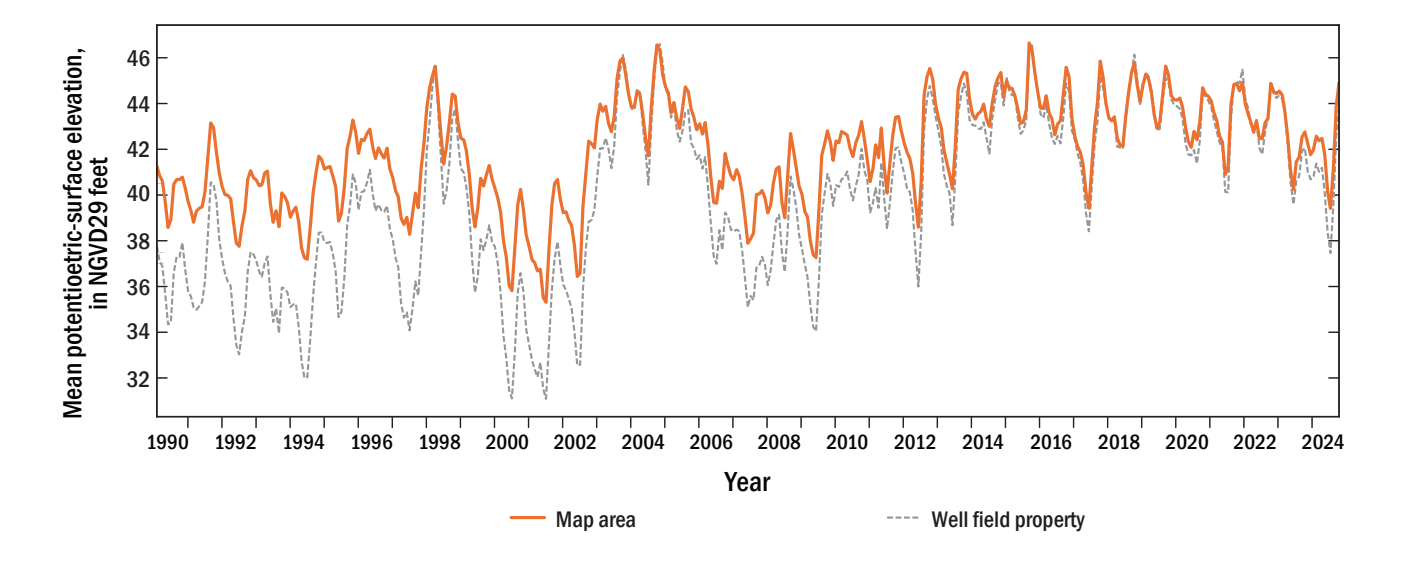


Figure 10. Spatially averaged monthly potentiometric-surface elevation for the map area and for the area inside the eight well-field properties, from January 1990 to September 2024.

Mean absolute cross-validation errors for wells in the network were generally lower for the eight-year and ninemonth extension than for the 26 years evaluated by Lee and Fouad (2017). In that evaluation, nine fewer wells had 2 feet or less mean monthly absolute cross-validation error, and seven more wells (15 total) had greater than 6 feet of error (Lee and Fouad, 2017). Mean crossvalidation errors in the 26-year study were also higher than in the ten years studied by Lee and Fouad (2014; fig. 15). In both cases, the comparatively smaller mean absolute cross-validation errors likely reflect comparing a shorter time period to the broader range of well-field pumping conditions encountered over the 26-year period. The effect of pumping on the cross-validation error, and correspondence between pumping and cross-validation error was described further in Lee and Fouad (2017; fig. 13) and Lee and Fouad (2014; fig. 16).

Curve-fit parameters used to create the semivariogram models for kriging the monthly potentiometric surfaces, namely the nugget, range, and sill, are summarized in Supplemental Data 4. Magnitudes of these parameters also exhibited a temporal correspondence to pumping withdrawals from Tampa Bay Water well fields in an earlier study, and fluctuated monthly in response to wetter and drier seasonal climate and pumping conditions (Lee and Fouad, 2014; figs. 16 and 17).

Monthly-Average Potentiometric Surfaces

The minimum and maximum monthly potentiometric surfaces within the eight-year and nine-month extension are shown in figure 9 along with an average surface for that period (fig. 9). The potentiometric surface reached a maximum elevation in September 2017, and a minimum in June 2024, a monthly pattern consistent with previous studies, and an annual pattern consistent with the overall

declining trend in groundwater elevations during the study period. The maximum pixel elevation to occur in the maximum potentiometric surface was 89.0 feet and the lowest pixel elevation in the minimum potentiometric surface was 0.4 feet.

During the previous 26 years the minimum and maximum potentiometric surfaces also occurred in June and September, respectively. A minimum pixel elevation of 0.6 feet occurred in the minimum surface in June 2001, and a maximum pixel elevation of 91.7 feet occurred in September 2004 and was 2.7 feet higher than the maximum in September 2017 (Lee and Fouad, 2017). The entire time series of 417 gridded surfaces, mapping the monthly-average potentiometric surfaces in the Upper Floridan aquifer across three decades is online at https://www.swfwmd.state.fl.us/resources/data-maps/hydrologic-data under the heading "Other Hydrologic Data Sources."

All of the pixel elevations in the 573-square-mile potentiometric-surface map area were averaged to create a spatially averaged monthly elevation. September 2017 had the highest spatial average elevation for the entire mapping area (45.9 feet) and June 2024 had the lowest (39.4 feet) (fig. 10). These months are mapped in figure 9.

Seasonal elevation extremes, which trended upward between 2006 and 2015, have trended downward overall from January 2016 to June 2024 (fig. 10). The average potentiometric surface elevation rose steeply in September 2024 to 44.9 feet and would likely continue to rise in October 2024 due to rainfall from Hurricane Milton on October 9, 2024.

The September and May/June timing of seasonal highs and lows, respectively, were consistent across the entire 34-year and nine-month record. September 2004 and September 2015 nearly match for period of record highs at 46.6 and 46.3 feet, respectively (fig. 10). The lowest average potentiometric-surface elevation of the past 34 years and

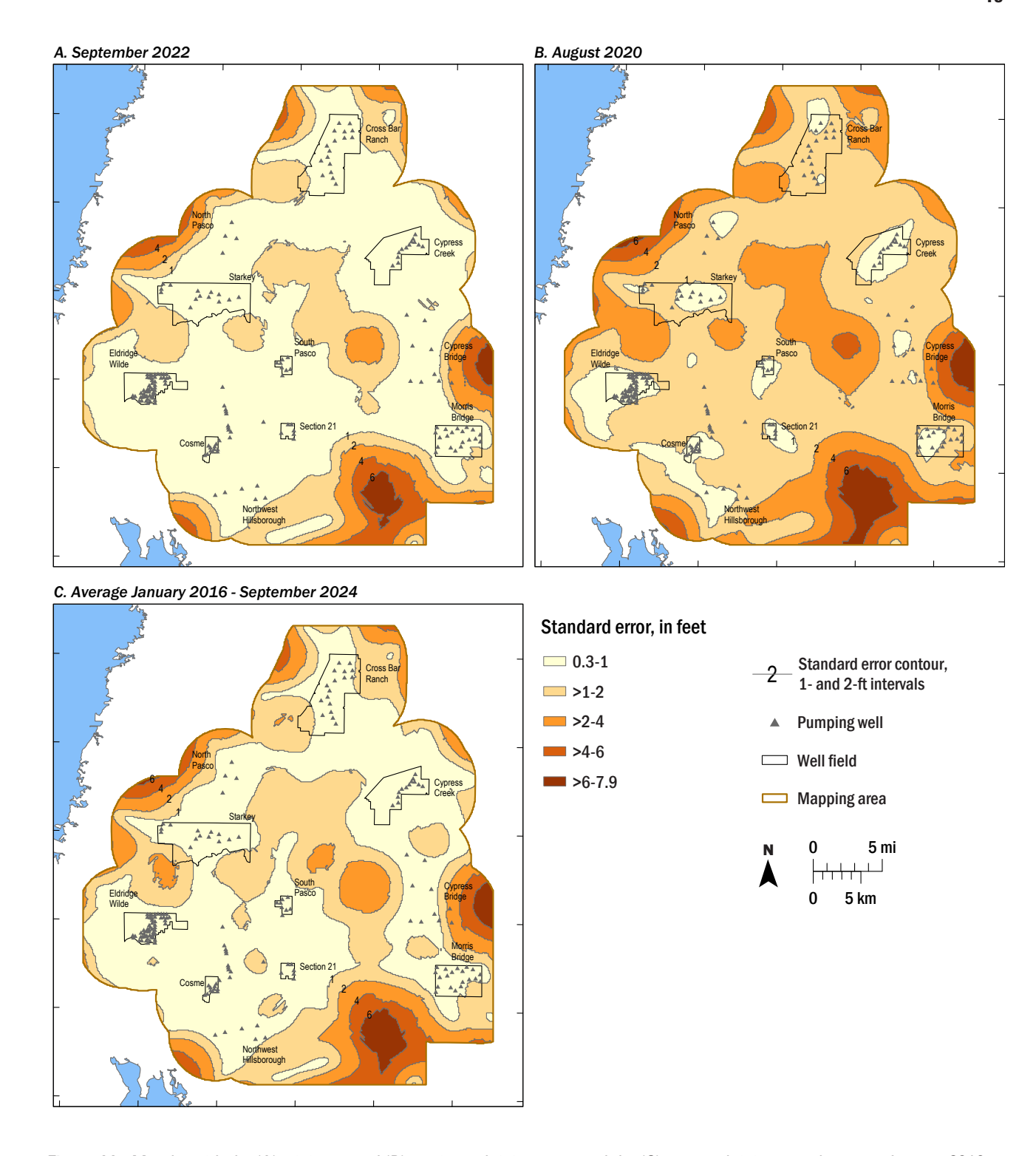


Figure 11. Months with the (A) minimum and (B) maximum kriging error, and the (C) average kriging error between January 2016 and September 2024.

nine months occurred in June 2001 followed by June 2000, prior to pumping cutbacks and with both extremes part of the same drought (Lee and Fouad, 2017; Verdi et al., 2006).

Historically, especially before pumping cutbacks, the average elevation inside well field properties (combined area 50.4 square miles) tracked 2 to 4 feet below the average elevation in the greater map area (fig. 10). After cutbacks,

and specifically between late 2012 and early 2023, monthly average elevations in both areas tracked closely through time. During 2023 and 2024 the difference in average elevations for the two areas increased noticeably, reaching 1.9 feet in June 2024 (fig. 10).

Contours of elevation drawn at five-foot intervals on the potentiometric surface maps appear jagged and angular

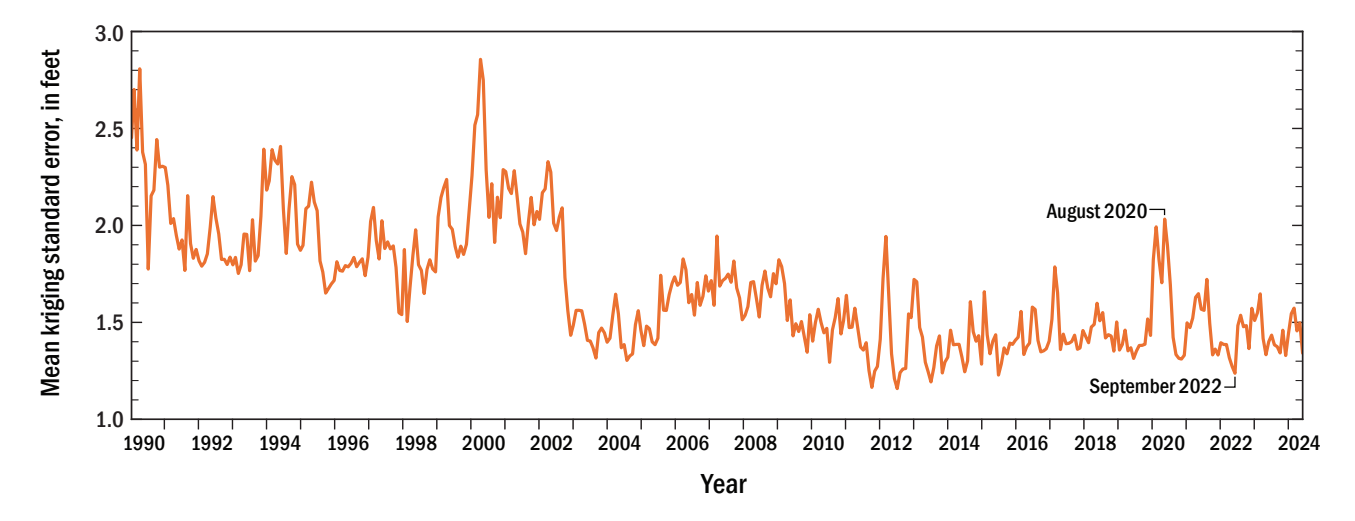


Figure 12. Spatially averaged monthly kriging error for the map area from January 1990 to September 2024.

in the far southeast corner. Some of these contours extend into the southern part of Morris Bridge well field, others extend southwest from there (fig. 9). The appearance of these contours reflects the limits of the kriging method to interpolate potentiometric surface elevations in areas where monitoring wells are scarce. Elsewhere on the map, where more data were available, monthly contours appear smooth and show uniformity with neighboring contour lines (fig. 9). This same result was evident in Lee and Fouad (2017, fig. 15). As discussed in the following section, it is also why the kriging error in the southeastern area of the map was larger than elsewhere in the map.

Uncertainty in the Monthly-Average Potentiometric Surfaces

The spatial distribution of kriging standard errors provides an estimate of uncertainty in the monthly potentiometric-surface elevations. The spatially distributed standard error from January 2016 to September 2024 varied monthly with pixel values ranging from a minimum of 0.3 feet to a maximum of 7.9 feet (fig. 11). The range was smaller than that for the previous mapping time period from 1990 to 2015 (Lee and Fouad, 2017), which varied from 0.2 to 10.6 feet.

Kriging standard errors reflect the degree of spatial variance in the monthly-average groundwater levels. In general, the greater the degree of "unevenness" in the potentiometric surface, the greater the spatial variance, and the larger the standard errors. Thus, standard errors tend to be greater in drier months with more groundwater pumping, which probably explains why the greater groundwater pumping during the 26-year mapping period resulted in greater standard errors. In months when the potentiometric surface is higher and smoother, such as wetter months with less groundwater pumping, spatial variance and standard errors tend to be less.

During the new period, September 2022 had the minimum spatially averaged standard error and August 2020 had the maximum spatially averaged standard error. The average standard error for the period is shown

for comparison (fig. 11). The largest standard errors consistently occured in the southeast region of the map where a single well exists at the far southern edge (see the southernmost red marker in fig. 3). Further, the well had been deactivated, and the study relied on creating synthetic data at this site.

Standard errors were also large near the Cypress Bridge well field at the eastern margin of the map, again where monitoring wells are scarce (fig. 3). Kriging standard errors in excess of four feet occur predictably around the margins of the mapping area where monitoring wells are not present. In contrast, kriging standard errors were small, mostly less than a foot on average, in and around well fields where more monitoring wells exist and potentiometric-surface elevations could be mapped with greater certainty (fig. 11).

Kriging standard errors, like the potentiometric surface, can be averaged over the entire mapping area and plotted over time (fig. 12). This shows that although the current mapping period has smaller standard errors than distant prior time periods like the 1990s, the present period has a slight upward trend in kriging standard errors with some notable peaks in the present decade that exceed those in the prior decade (i.e., compare 2020s to 2010s). The peaks are not linked to the gap-filling (fig. 5) as one might presume since August 2020, the month of greatest standard error in the present decade, does not have an exceptionally large percentage of gap-filled record compared to other months. Rather, the increase in standard error more closely corresponds to the slight uptick in groundwater pumping (fig. 2b) that can again induce more local variability in potentiometric-surface elevations and lead to larger kriging standard errors. Drier conditions (fig. 2a) may also be a contributing factor in increasing standard errors as in prior studies a notable drought (Verdi et al., 2006) was linked to the month of greatest average standard error (Lee and Fouad, 2014 and 2017).

The Final Spatial Extent of the Mapping Time Series

The kriging analysis interpolated the potentiometric surface elevations across a rectangular region of the Northern Tampa Bay area (fig. 1). However, the published time series of the potentiometric surface in the Upper Floridan aguifer is a lobe-shaped area clipped from the rectangular raster grids (fig. 3). This map area centers on the 11 well-field properties, where the concentration of monitoring wells is densest and the kriging standard errors are smallest (fig. 11). The 573-square-mile map area encompasses numerous surface-water features in the Northern Tampa Bay area, including lakes and wetlands, and parts of six stream drainage basins including the Anclote River, Pithlachascotee River, Cypress Creek-Hillsborough River, Middle Hillsborough River, Rocky Creek-Sweetwater Creek, and Moccasin Creek-Double Branch. To increase the versatility of the mapping layers, the boundaries of the mapped area could be expanded to encompass selected surface-water features if the uncertainty in the added data were acceptable.

For example, Tampa Bay Water and the Southwest Florida Water Management District each have a regulatory responsibility to assess the hydrologic status of unmonitored wetlands subject to the effects of groundwater pumping under the Consolidated Water Use Permit (11771.002) reissued in 2022 through the year 2032. A large number of wetlands, some 10,000 plus (Fouad and Lee, 2021), fall within the map area of the final time series, a large sample for expansive studies of unmonitored wetlands and their hydrologic response to changes in climate and pumping regimes.

Study results generated several recommendations to Tampa Bay Water to maintain and improve the monitoring well network and future mapping products. The first recommendation is to take over monitoring duties for Bexley Well 2 Near Drexel FL where the USGS is scheduled to discontinue monitoring on October 1, 2025 according to the Water Data for the Nation website. The second recommendation is to do an evaluation study to optimize the existing well network. A fraction of the wells in the current well network may be providing redundant data that does little to improve the accuracy of the mapping product. An optimization study can identify redundant wells so that their inclusion in the network can be evaluated by Tampa Bay Water and expensive and time consuming monitoring at redundant wells may be reassigned to other well locations in the Northern Tampa Bay area. Labor and cost savings could be directed toward drilling new wells, or establishing cooperative agreements to monitor exising wells. For instance, this could happen at wells drilled by the USGS in the Temple Terrace well field (Katz et al., 2007) where observations are currently absent from the monitoring network.

Summary

This study generated digital data layers describing the monthly average potentiometric-surface elevations in the

Upper Floridan aquifer in the Northern Tampa Bay area of Florida over 34 years and nine months, from January 1990 to September 2024. A complementary series of data layers quantifies the kriging standard error, or uncertainty, associated with the elevations. Because the mapping time series spans multiple decades, it can be used to analyze the effects of changing climate and well-field operations on the region's hydrology. The highly spatially resolved potentiometric-surface maps can be used to track changes in the groundwater levels of the Upper Floridan aquifer through time, and corresponding changes in the hydrologic setting of overlying wetlands, lakes, and streams.

Study results include a summary of available raw data for the 195 monitoring wells used in this analysis, and daily and monthly-averaged gap-filled time series for each well. The interpolation methods used in this report are those of Lee and Fouad (2017), originally adapted from Lee and Fouad (2014). This study reapplies the methods of Lee and Fouad (2017) to extend the mapping time series by eight years and nine months from January 2016 to September 2024. This report uses the same naming and numbering conventions to identify wells as Lee and Fouad (2014 and 2017). This allows all of the site maps and tables in the first two reports to extend to the current report and makes it easy for the reader to access the in-depth discussions of prior studies on many of the topics touched upon in this extended analysis.

References Cited

- Carter, L., Terando, A., Dow, K., Hiers, K., Kunkel, K.E., Lascurain, A., Marcy, D., Osland, M., and Schramm, P., 2018, Southeast. In: Impacts, Risks, and Adaptation in the United States: Fourth National Climate Assessment, Volume II [Reidmiller, D.R., Avery, C.W., Easterling, D.R., Kunkel, K.E., Lewis, K.L.M., Maycock, T.K., and Stewart, B.C. (eds.)]. U.S. Global Change Research Program, Washington, DC, USA, pp. 743–808. https://repository.library.noaa.gov/view/noaa/19487/noaa 19487 DS1.pdf.
- Conrads, P.A., Petkewich, M.D., O'Reilly, A.M., and Telis, P.A., 2014, Hydrologic record extension of water-level data in the Everglades Depth Estimation Network (EDEN), 1991–99: U.S. Geological Survey Scientific Investigations Report 2014-5226, 27 p. http://dx.doi.org/10.3133/sir20145226.
- Efron, B., and Tibshirani, R., 1997, Improvements on cross-validation: The .632+ bootstrap method. Journal of the American Statistical Association, 92(438). https://doi.org/10.2307/2965703.
- Fisher, J.C., 2013, Optimization of water-level monitoring networks in the Eastern Snake River Plain Aquifer using a kriging-based genetic algorithm method: U.S. Geological Survey Scientific Investigations Report 2013-5120, 74 p. https://doi.org/10.3133/sir20135120.
- Florida Climate Center, 2024, Post-storm summary report on Hurricane Milton, Florida State University Center for Ocean Atmospheric Prediction Studies, 12 p. https://climatecenter.fsu.edu/images/docs/Hurricane-Milton-Report.pdf.
- Fouad, G., and Lee, T.M., 2021, A spatially distributed groundwater metric for describing hydrologic changes in a regional population of wetlands north of Tampa Bay, Florida, from 1990 to 2015. Wetlands, 41(103). https://doi.org/10.1007/s13157-021-01502-w.
- Geurink, J.S., and Basso, R., 2013, Development, calibration, and evaluation of the Integrated Northern Tampa Bay Hydrologic Model, prepared by Tampa Bay Water, Clearwater, FL, and the Southwest Florida Water Management District, Brooksville, FL, 916 p.
- Haag, K.H. and Lee, T.M., 2010, Hydrology and ecology of freshwater wetlands in central Florida—A primer: U.S. Geological Survey Circular 1342, 138 p. https:// pubs.usgs.gov/circ/1342/.
- Hogg, W., Hayes, E., Keesecker, D., Kiehn, W., and Shea, C., 2020, Tampa Bay Water recovery assessment: Final report of findings, prepared by Tampa

- Bay Water, Clearwater, FL, 859 p. https://www.tampabaywater.org/wp-content/uploads/Recovery-Assessment-Final-Report-of-Findings.pdf.
- Interlocal Agreement, 1998, Amended and restated interlocal agreement reorganizing the west coast regional water supply authority. State of Florida legal document, 116 p. https://ufdc.ufl.edu/WL00003978/00001.
- Katz, B.G., Crandall, C.A., Metz, P.A., McBride, W.S., and Berndt, M.P., 2007, Chemical characteristics, water sources and pathways, and age distribution of ground water in the contributing recharge area of a public-supply well near Tampa, Florida, 2002-05, US Geological Survey Scientific Investigation Report 2007-5139, 83 p. https://pubs.usgs.gov/publication/ sir20075139.
- Lee, T.M., Haag, K.H., Metz, P.A., and Sacks, L.A., 2009, The comparative hydrology, water quality, and ecology of selected natural and augmented freshwater wetlands in west-central Florida: U.S. Geological Survey Professional Paper 1758, 152 p. https://pubs.usgs.gov/pp/1758/.
- Lee, T.M., and Fouad, G.G., 2014, Creating a monthly time series of the potentiometric surface in the Upper Floridan Aquifer, Northern Tampa Bay area, Florida, January 2000-December 2009. US Geological Survey Scientific Investigations Report 2014-5038, 26 p. Report and data products available at https://pubs.usgs.gov/sir/2014/5038/.
- Lee, T.M., and Fouad, G.G., 2017, Extending the monthly time series of the potentiometric surface in the Upper Floridan aquifer, Northern Tampa Bay area, Florida, January 1990-December 2015. Report for Tampa Bay Water, Clearwater, FL, 30 p. Report and data products available under Other Hydrologic Data Sources at https://www.swfwmd.state.fl.us/resources/data-maps/hydrologic-data.
- Lee, T.M., and Fouad, G., 2018, Changes in wetland groundwater conditions in the Northern Tampa Bay area from 1990 to 2015. Report for Tampa Bay Water, Clearwater, FL, 56 p. Report and data products available under Other Hydrologic Data Sources at https://www.swfwmd.state.fl.us/resources/data-maps/hydrologic-data.
- Lee, T.M., Sacks, L.A., and Hughes, J.D., 2010, Effects of groundwater levels and headwater wetlands on streamflow in the Charlie Creek Basin, Peace River watershed, west-central Florida: U.S. Geological Survey Scientific Investigations Report 2010–5189, 77 p. https://pubs.usgs.gov/sir/2010/5189/.

- Sinclair, W.C., Knutilla, R.L., Gilboy, A.E., and Miller, R.L., 1985, Types, features, and occurrence of sinkholes in the karst of west-central Florida. U.S. Geological Survey Water-Resources Investigations Report 85-4126, 81 p. https://doi.org/10.3133/ wri854126.
- Southwest Florida Water Management District, 1999, Establishment of recovery levels in the Northern Tampa Bay area: Brooksville, Southwest Florida Water Management District report, 237 p.
- Southwest Florida Water Management District, 2024, Hydrologic Conditions for the month of May 2024, Hydrologic Data Section, Brooksville, FL, June 25, 2024, 72 p., accessed from https://www.swfwmd.state.fl.us/resources/weather-hydrology/hydrologic-conditions-reports at https://www.swfwmd.state.fl.us/sites/default/files/medias/documents/HCR_May 2024 internet.pdf.
- Southwest Florida Water Management District, 2025a, Water Management Information System, Water Use Permit Information, Landscape/recreation permits available at https://www18.swfwmd.state.fl.us/search/search/search/wupsimple.aspx.
- Southwest Florida Water Management District, 2025b, Rainfall summary data by region, USGS watershed (matrix) available at https://www.swfwmd.state.fl.us/ resources/data-maps/rainfall-summary-data-region.
- Southwest Florida Water Management District, 2025c, Hydrologic Conditions for the month of May 2025, Hydrologic Data Section, Brooksville, FL, June 24, 2025, 72 p., accessed from https://www.swfwmd.state.fl.us/resources/weather-hydrology/hydrologic-conditions-reports at https://www.swfwmd.state.fl.us/sites/default/files/medias/documents/HCR_May_2025_internet.pdf.
- Tampa Bay Water, 2013, Defining areas of investigation for recovery analysis. Tampa Bay Water, Clearwater, FL, 22 p.
- Verdi, R.J., Tomlinson, S.A., and Marella, R.L., 2006, The drought of 1998–2002: Impacts on Florida's hydrology and landscape: U.S. Geological Survey Circular 1295, 34 p. https://doi.org/10.3133/cir1295.
- White, W.A., 1970, The Gulf Coastal Lowlands. In: The Geomorphology of the Florida Peninsula. Florida Bureau of Geology Geological Bulletin No. 51, pp. 142-155. http://ufdc.ufl.edu/UF00000149/00001.

Williams, L.J., and Kuniansky, E.L., 2016, Revised hydrogeologic framework of the Floridan aquifer system in Florida and parts of Georgia, Alabama, and South Carolina: U.S. Geological Survey Professional Paper 1807, 140 p., https://doi.org/10.3133/pp1807.